

# Integrative genomic analyses identify *MITF* as a lineage survival oncogene amplified in malignant melanoma

Levi A. Garraway<sup>1,3</sup>, Hans R. Widlund<sup>1</sup>, Mark A. Rubin<sup>2,3</sup>, Gad Getz<sup>5</sup>, Aaron J. Berger<sup>6</sup>, Sridhar Ramaswamy<sup>5,7</sup>, Rameen Beroukhi<sup>1,3</sup>, Danny A. Milner<sup>2,3</sup>, Scott R. Granter<sup>2</sup>, Jinyan Du<sup>1,5</sup>, Charles Lee<sup>2,3</sup>, Stephan N. Wagner<sup>8</sup>, Cheng Li<sup>1,4</sup>, Todd R. Golub<sup>1,3,5</sup>, David L. Rimm<sup>6</sup>, Matthew L. Meyerson<sup>1,2,5</sup>, David E. Fisher<sup>1,3</sup> & William R. Sellers<sup>1,2,3,5</sup>

Systematic analyses of cancer genomes promise to unveil patterns of genetic alterations linked to the genesis and spread of human cancers. High-density single-nucleotide polymorphism (SNP) arrays enable detailed and genome-wide identification of both loss-of-heterozygosity events and copy-number alterations in cancer<sup>1–5</sup>. Here, by integrating SNP array-based genetic maps with gene expression signatures derived from NCI60 cell lines, we identified the melanocyte master regulator *MITF* (microphthalmia-associated transcription factor) as the target of a novel melanoma amplification. We found that *MITF* amplification was more prevalent in metastatic disease and correlated with decreased overall patient survival. *BRAF* mutation and p16 inactivation accompanied *MITF* amplification in melanoma cell lines. Ectopic *MITF* expression in conjunction with the *BRAF*(V600E) mutant transformed primary human melanocytes, and thus *MITF* can function as a melanoma oncogene. Reduction of *MITF* activity sensitizes melanoma cells to chemotherapeutic agents. Targeting *MITF* in combination with *BRAF* or cyclin-dependent kinase inhibitors may offer a rational therapeutic avenue into melanoma, a highly chemotherapy-resistant neoplasm. Together, these data suggest that *MITF* represents a distinct class of ‘lineage survival’ or ‘lineage addiction’ oncogenes required for both tissue-specific cancer development and tumour progression.

To begin to organize human cancers on the basis of large-scale chromosomal alterations, we first evaluated the genomes of NCI60 cell lines<sup>6</sup> using pre-release 100K SNP arrays (Affymetrix). These arrays interrogate over 124,000 SNP alleles spaced with a median intermarker distance of 8.5 kilobases (kb). The NCI60 cell lines represent tumours from nine different tissue types and are annotated by multiple large-scale data sets<sup>7–10</sup>. Thus, these cell lines offer a platform for testing integrated and orthogonal analytic approaches (Fig. 1a). The complete NCI60 SNP array data are available at [http://dtp.nci.nih.gov/mtargets/mt\\_index.html](http://dtp.nci.nih.gov/mtargets/mt_index.html) and at <http://www.ncbi.nlm.nih.gov/geo> (accession number GSE2520).

To determine whether patterns of copy number alterations identified distinct genetic subgroups, hierarchical clustering<sup>11</sup> was used to organize 58 NCI60 cell lines based on copy-number alterations defined by SNP array analysis (see Methods). The resulting dendrogram contained subclusters in which the samples segregated largely according to tissue of origin (Fig. 1b, Supplementary Fig. 1). One

such group consisted of lung cancer lines, another mainly of colon tumour lines, and another of cell lines derived from malignant melanoma (Fig. 1b). For each of these cell line clusters, there were also associated SNP clusters derived from contiguous chromosomal regions (Fig. 1b and Supplementary Fig. 1).

The tissue-based organization of the samples raised the possibility that the associated chromosomal aberrations might harbour lineage-specific cancer genes. To investigate this, we focused on a region of copy gain on chromosome 3 at 3p13–3p14 that defined the melanoma subcluster (Fig. 1b,c). Here, supervised analysis<sup>12</sup> (see Supplemental Methods) was performed using available NCI60 gene expression data, looking for gene expression correlates of the class distinction ‘3p amplified’ (six melanoma cell lines) versus ‘3p non-amplified’ (remaining NCI60 lines; Fig. 1c). 583 transcripts demonstrated significantly increased expression in the 3p-amplified class after Bonferroni correction, with  $P < 10^{-6}$  by *t*-statistic. This expression signature was influenced significantly by lineage-related differences in transcript profiles between melanomas and the other NCI60 tissue types, as noted by others<sup>7</sup>. Nonetheless, only one highly expressed gene, *MITF*, was located within the amplified region ( $t$ -ratio = 17.36,  $P$ -value =  $2.97 \times 10^{-12}$ , adjusted threshold for significance =  $3.96 \times 10^{-6}$ ; Figs 1c, d). In a similar analysis restricted to just the eight NCI60 melanoma cell lines, the mean *MITF* expression ratio between the 3p-amplified (six samples) and non-amplified (two samples) classes exceeded that of nearly all randomly permuted class distinctions (data not shown). *MITF* encodes a basic helix–loop–helix/leucine zipper transcription factor required for development of the melanocyte lineage<sup>13</sup>, but not previously known to be the target of an acquired somatic mutation. These data raised the possibility that *MITF* might also function as a lineage-specific oncogene.

We then investigated *MITF* gene dosage in human tumours by performing quantitative polymerase chain reaction (PCR) on DNA derived from a series of melanocytic nevi, primary cutaneous melanomas, and melanoma metastases. *MITF* amplification was observed in 3 of 30 (10%) primary cutaneous and 7 of 32 (21%) metastatic tumours, but not in the ten benign nevi tested (Fig. 2a). *MITF* was the most consistently amplified gene in the ‘core’ amplified region defined by MALME-3M cells (Fig. 1d) and, when amplified to high levels, appeared to represent the epicentre of the amplicon (see,

<sup>1</sup>Departments of Medical Oncology, Pediatric Oncology, Biostatistical Sciences and Melanoma Program in Medical Oncology, Dana-Farber Cancer Institute, 44 Binney Street,

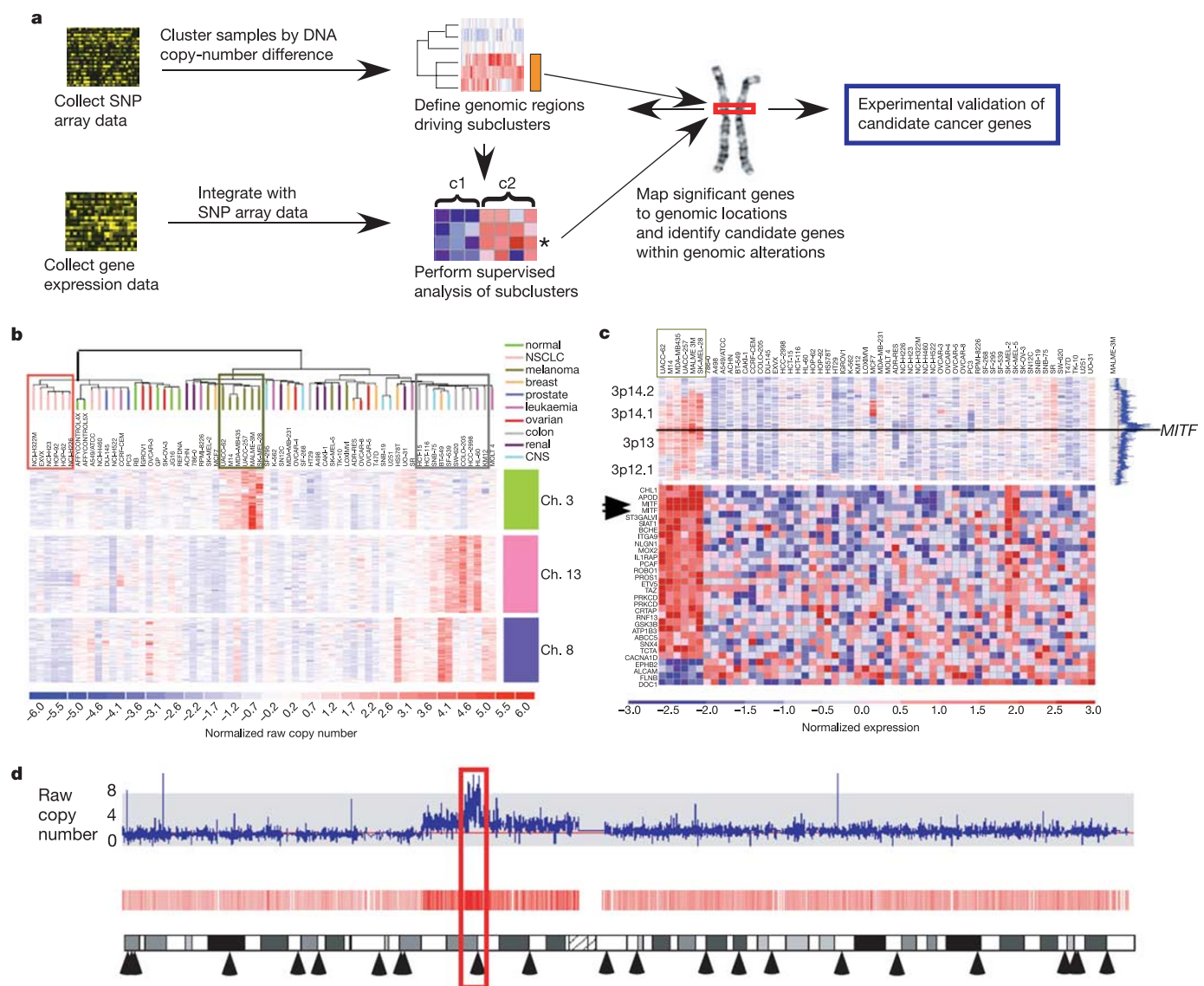
<sup>2</sup>Departments of Pathology, Brigham and Women’s Hospital and Harvard Medical School, <sup>3</sup>Department of Medicine, Brigham and Women’s Hospital, Harvard Medical School, 75 Francis Street, <sup>4</sup>Department of Biostatistics, Harvard School of Public Health, 677 Huntington Avenue, Boston, Massachusetts 02115, USA. <sup>5</sup>The Broad Institute of Harvard and MIT, 320 Charles Street, Cambridge, Massachusetts 02141, USA. <sup>6</sup>Department of Pathology, Yale University School of Medicine, 310 Cedar Street, New Haven, Connecticut 06510, USA. <sup>7</sup>Massachusetts General Hospital Center for Cancer Research and Department of Medicine, 149 13th Street, Charlestown, Massachusetts 02129, USA. <sup>8</sup>DIAD, Department of Dermatology, Medical University of Vienna, and Center of Molecular Medicine, Austrian Academy of Sciences, Währinger Gürtel 18–20, A-1090 Vienna, Austria.

for example, samples IM3 and MM5; Fig. 2c). Together, these data delineated *MITF* as the probable oncogene targeted by this genetic alteration.

Next, we examined nearly 200 tissue specimens derived from primary and metastatic melanomas by fluorescence *in situ* hybridization (FISH) using bacterial artificial chromosome (BAC) probes spanning the *MITF* locus (to detect extra-chromosomal amplification events). *MITF* amplification (range = 4–13 copies per cell; Fig. 3b and Supplementary Table 3) was detected in 2 of 19 (10.5%) cutaneous tumours and 27 of 160 (15.2%) metastatic samples. Once again, no amplification was detected in nine melanocytic nevi analysed. In metastatic melanoma, *MITF* amplification was associated with decreased 5-year survival (Fig. 3c; Kaplan–Meier log rank  $P$  value = 0.024), but not with other clinicopathologic parameters (Supplementary Figs 2 and 3). *MITF* protein levels were also analysed in the melanoma tissue microarray using automated quantitative analysis (AQUA) technology<sup>14</sup>. *MITF* amplification

correlated with a significantly increased mean *MITF* protein expression in metastatic disease ( $P = 0.019$ ; Figs 3d–f). This association remained significant when expression was measured as a continuous variable in relation to *MITF* copy number (data not shown). Together, these observations implicate *MITF* amplification in the progression and lethality of a subset of human melanomas.

In melanocytes, activated MAP kinase triggers *MITF* phosphorylation at serine-73 (ref. 15), recruiting the transcriptional coactivator p300 (ref. 16) while simultaneously targeting *MITF* for ubiquitin-dependent proteolysis<sup>17</sup>. Normal melanocyte growth/differentiation may also require the coordinated actions of *MITF* and cyclin-dependent kinase (CDK) inhibitors such as p16 or p21 (refs 18, 19). On the other hand, aberrant MAP kinase signalling through activating *BRAF* or *NRAS* mutations may underlie a substantial percentage of melanomas<sup>20,21</sup>. Interestingly, all NCI60 cell lines harbouring *MITF* copy gain also contained both the *BRAF*(V600E) mutation and p16 pathway inactivation<sup>22</sup> (Supplementary Table 2). Thus,



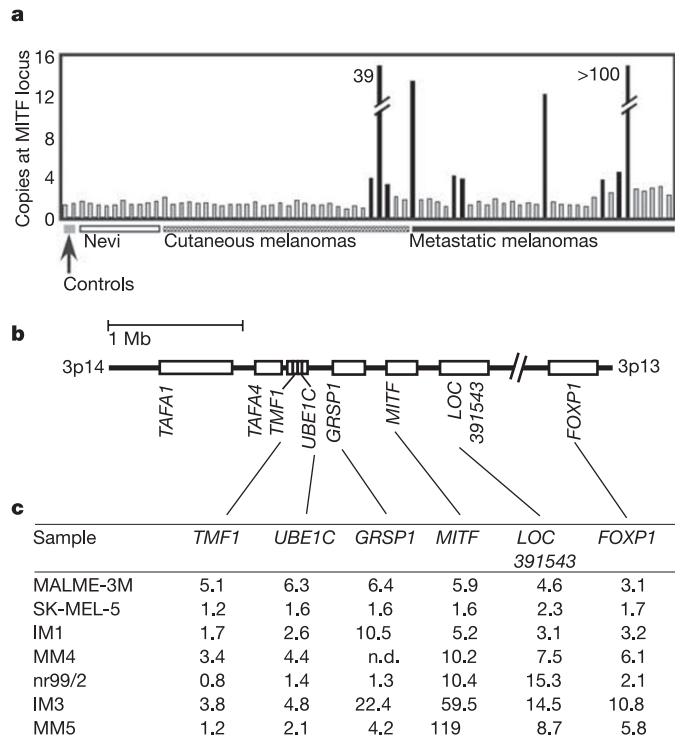


**Figure 2** | *MITF* maps to the epicentre of an amplicon present in a subset of malignant melanomas. **a**, Quantitative PCR analysis of the *MITF* locus across 62 benign nevi, primary and metastatic melanomas. Cases with *MITF* amplification are shaded black. **b**, Transcript map of the core 3p13–3p14 amplicon present within the MALME-3M cell line. The *FOXP1* gene resides outside the core amplicon. **c**, Quantitative PCR analysis of several genes within the amplicon (see Methods for details). MALME-3M and SK-MEL-5 are NCI60 cell lines with and without the amplicon, respectively. IM1 and IM3 are primary melanoma samples; MM4, MM5 and nr 99/2 are metastatic melanoma samples. *TMF1*, *UBE1C*, *GRSP1*, *LOC391543* and *FOXP1* are genes flanking *MITF*.

genetic amplification of *MITF* might promote tumour formation and/or survival in the setting of cell cycle deregulation and excess MAP kinase pathway activation.

To test this hypothesis *in vitro*, we sought to overexpress *MITF* in

genetically modified human melanocytes. In these cells, p53 and p16/CDK4/RB (where RB is the retinoblastoma protein) pathways were inactivated in conjunction with telomerase (hTERT) expression (hTERT/CDK4(R24C)/p53DD melanocytes; see Supplementary Methods). Though characterized by a markedly extended proliferative capacity (>1.5 years in culture), these cells require both TPA (12-*O*-tetradecanoylphorbol-13-acetate) and cyclic (c)AMP agonists for survival (a hallmark of non-transformed melanocytes).

Next, these modified melanocytes were transduced with either empty retrovirus or retroviruses directing the expression of BRAF(V600E) or *MITF* (Figs 4a, b). In the presence of TPA and dibutyryl cAMP (dbcAMP), *MITF* did not alter the growth of these melanocytes, although BRAF(V600E) expression was incompatible with these factors (data not shown). In the absence of TPA and cAMP agonists, neither vector control nor *MITF* expression alone had any effect on melanocyte growth factor requirements (Fig. 4a). Notably, ectopic BRAF(V600E) expression was associated with loss of *MITF* protein (Fig. 4b), and enabled minimal factor-independent growth (Fig. 4a). Both primary and hTERT/CDK4(R24C)/p53DD melanocytes showed identical *MITF* and wild-type BRAF protein levels (not shown). In contrast, the expression of *MITF* together with activated BRAF conferred robust factor-independence (Fig. 4a). BRAF(V600E) and haemagglutinin (HA)-tagged *MITF* co-expression was associated with enrichment of the upper band near 60 kilodaltons (kDa) (Fig. 4b) shown previously to represent the serine-73 phosphorylated variant associated with *MITF* activation<sup>15,23</sup>. When the same cells were suspended in soft agar, only cells expressing both BRAF(V600E) and HA-*MITF* formed anchorage-independent colonies (Figs 4c, d). Thus, deregulated *MITF* expression cooperated with BRAF(V600E) to transform human melanocytes.

Genetic amplification of *MITF* also suggests that the melanocyte lineage dependency on *MITF* might be maintained in melanoma tumour cells<sup>23</sup>. To test this, an adenovirus expressing a dominant-negative *MITF* mutant<sup>23,24</sup> (Ad-dn*MITF*; see Methods) was introduced into NCI60 melanoma cell lines that exhibited varying levels of *MITF* amplification (Supplementary Fig. 4c). Growth of three NCI60 melanoma cell lines was inhibited following introduction of Ad-dn*MITF*; however, those with *MITF* copy gain were more refractory to the dn*MITF* effect (Fig. 4e). Similar results were also observed following short hairpin (sh)RNA-mediated *MITF* knock-down (data not shown). Inhibition of *MITF* function in melanoma cells may trigger CDK2-mediated growth arrest<sup>24</sup> or apoptosis

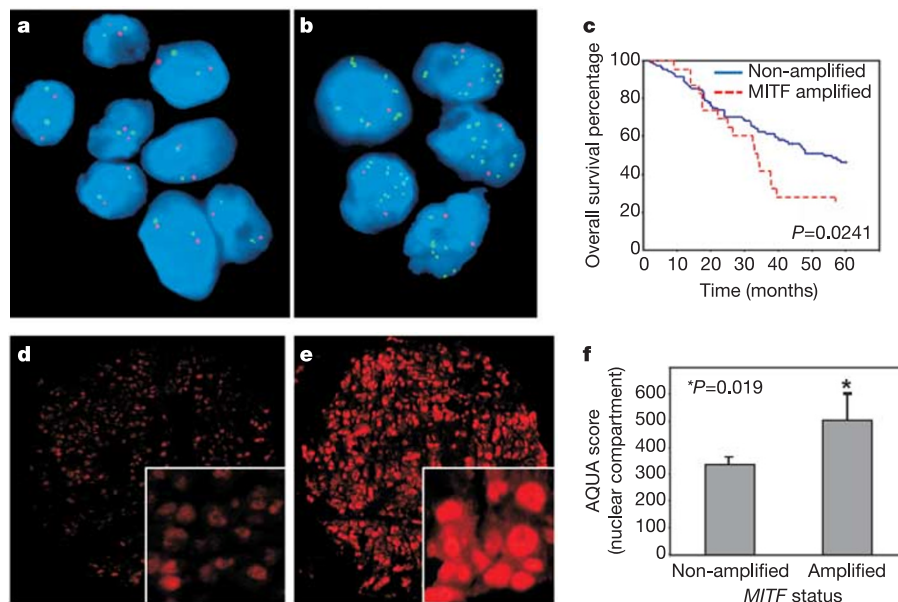


**Figure 3** | FISH, Kaplan-Meier and AQUA analysis of *MITF* in human melanoma samples. Green digoxin- and red SpectrumOrange (from Vysis)-labelled BAC probes detected the *MITF* locus and chromosome 3 centromere, respectively, in a melanoma tissue microarray. More than 50 nuclei were scored per amplified sample. **a**, **b**, A diploid case (**a**) and a case of *MITF* amplification (**b**) are shown. **c**, Kaplan-Meier survival analysis in metastatic melanoma patients with or without *MITF* amplification (log rank test,  $P = 0.024$ ). **d**, **e**, AQUA images for *MITF* protein levels in non-amplified and highly amplified samples ( $\geq 10$  copies per cell). **f**, Mean and standard error of AQUA scores for *MITF* protein in non-amplified (left) and amplified (right) metastatic melanoma samples.

though BCL2 downregulation<sup>23</sup>. Thus, these data suggest that deregulation of MITF through amplification or other mechanisms may preserve a critical lineage survival function in melanoma.

Melanocyte survival mechanisms that are modified by MITF may also contribute to melanoma chemoresistance<sup>23,25</sup>. To investigate whether *MITF* copy gain correlated with drug resistance, we performed a supervised analysis of the available NCI60 pharmacological data, where chemical sensitivity to a large number of small molecules and natural products is known (see Supplementary Methods). 3p copy gain was associated with a significantly increased mean GI50 in 270 compounds (median  $35 \pm 39.7$  compounds expected at random). This degree of chemoresistance was statistically significant within the overall NCI60 data set ( $P = 0.016$ ; Supplementary Fig. 5a, b). An analysis restricted to just the eight NCI60 melanoma cell lines revealed a similar trend, though this did not reach statistical significance with the limited available permutations (Supplementary Fig. 5c). To examine the specific effect of MITF on melanoma drug resistance, MALME-3M melanoma cells (which contain the *MITF* amplicon) were infected with Ad-dnMITF at sublethal multiplicity of infection (MOI) and cultured in the presence of commonly used chemotherapeutic agents. MALME 3M cells infected with empty adenovirus showed pharmacologic profiles similar to wild-type controls (Supplementary Fig. 5d). However, cells expressing dnMITF were significantly more susceptible to inhibition by 20  $\mu$ M of both cisplatin and docetaxel after 72 h (Fig. 4h). Drug titration curves also showed a four- to fivefold decrease in the cellular growth inhibitory concentration (GI<sub>50</sub>) of each agent in the presence of dnMITF (data not shown). Thus, reduction of MITF activity may sensitize melanomas to conventional chemotherapeutics.

Somatic alteration through gene amplification suggests that *MITF*

may be a member of a newly recognized 'lineage survival' or 'lineage addiction' oncogene subclass. Unlike oncogene addiction, where inappropriate gene-activation events render cells hyperdependent on particular pathways, dependency in this case might be pre-established during development and maintained in tumours through genetic aberrations. The androgen receptor (AR) is a prototype of this oncogene class that now includes *MITF*: both AR and MITF are required for the development and survival of their respective (prostate and melanocyte) lineages, maintained in cancers of these lineages, and amplified (or activated by mutation) in association with advanced disease. AR gene amplification typically occurs after androgen withdrawal therapy in prostate cancer patients. Although the cause of MITF amplification is not known, we speculate that increased MITF gene dosage (or deregulation by other means) may preserve its essential survival function in settings where the normal cues preserving MITF activity are lost. BRAF mutation and metastasis may constitute two such settings.

Although AR induces differentiation and growth arrest in non-transformed prostate epithelia in the presence of androgen, AR activation in the setting of p53 and Rb inactivation causes tumours in mice<sup>26</sup>. Similarly, MITF induces both differentiation and growth arrest in non-transformed cells<sup>18,19</sup>. Our results suggest that inactivation of p53 and Rb (the latter through loss of p16 activity) likewise enables MITF to transform human melanocytes in cooperation with mutated BRAF.

AR inhibition remains the most effective therapeutic intervention in prostate cancer, and emerging data suggests a continued dependency on AR in hormone-refractory disease<sup>27</sup>. Extending the lineage survival oncogene analogy, patient selection based on MITF, BRAF and p16 pathway mutation status might identify responders or

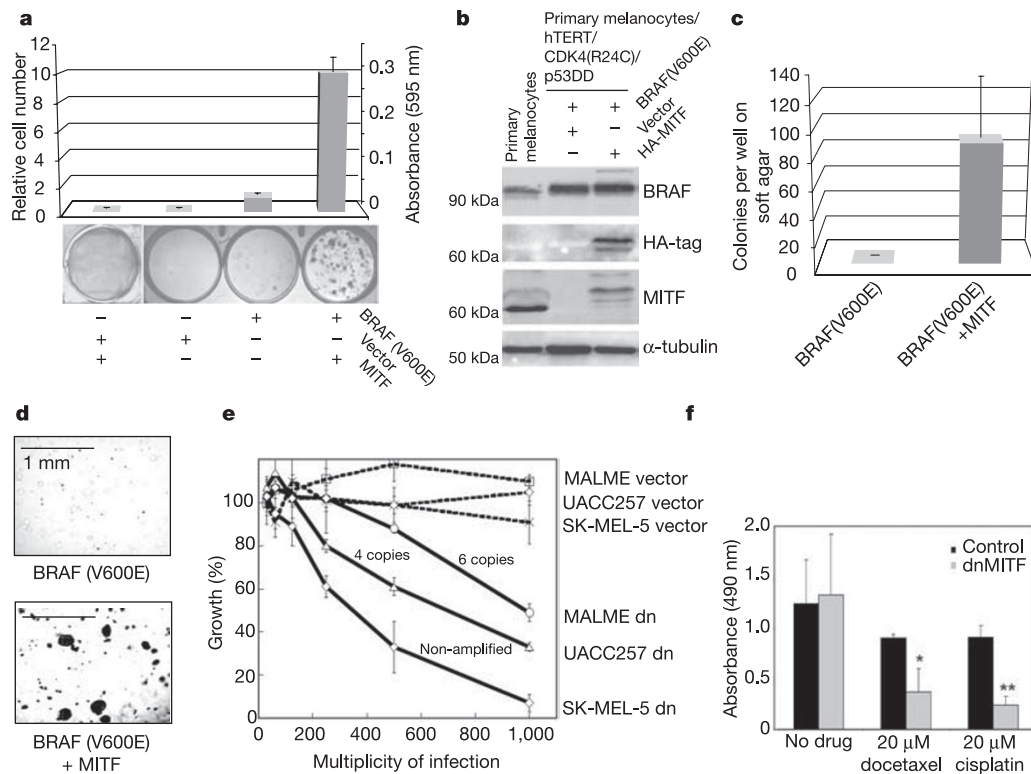


**Figure 4 | A role for deregulated MITF in melanoma tumorigenesis and survival.** **a**, MITF and BRAF(V600E) co-expression confers factor-independent growth in hTERT/CDK4(R24C)/p53DD melanocytes. Absorbance (mean and standard error) following crystal violet staining, and photographs at 3 weeks are shown. **b**, Extracts from hTERT/CDK4(R24C)/p53DD melanocytes expressing BRAF(V600E)  $\pm$  HA-MITF were immunoblotted using antibodies against BRAF, MITF, HA-tag or  $\alpha$ -tubulin. p53DD, dominant-negative p53. **c**, **d**, Growth of cells expressing

BRAF(V600E)  $\pm$  HA-MITF in soft agar. Colonies (mean and standard error) and photographs taken at 8 weeks are shown (magnification  $40\times$ ). **e**, Growth of melanoma cell lines expressing empty vector or dominant-negative MITF (dn) at 48 hours relative to uninfected controls. Means and standard deviations are shown; *MITF* copy number is indicated. **f**, Cell growth (mean and standard deviation, 72 h) of MALME-3M cells expressing dnMITF compared to uninfected controls, in the presence or absence of docetaxel or cisplatin (\* $P < 0.05$ , \*\* $P < 0.01$ ).

non-responders to the BRAF or CDK inhibitors currently in clinical development. Future combined genomic and functional studies may clarify tumour-survival mechanisms across many tumour types, thereby increasing biological understanding and providing new therapeutic possibilities.

## METHODS

**SNP array hybridization.** Genomic DNA from 58 NCI60 cell lines was obtained from R. Camalier and D. Scudiero of the National Cancer Institute Developmental Therapeutics programme (NCI DTP). All DNAs were quantified by Picogreen (Molecular Probes) before SNP array analysis. SNP array data collection, normalization and copy-number determination are described in the Supplementary Information.

**Hierarchical clustering using raw copy number data.** Raw copy number data from CentXba arrays was filtered to reduce invariant SNPs using dChipSNP software (available at <http://www.dchip.org>) by adjusting parameters for the values of standard deviation/mean. Filtered SNPs were subjected to hierarchical clustering using the Pearson coefficient and average linkage method<sup>11</sup>. Two-dimensional dendrograms (one for cell lines and one for SNPs) were generated (the full two-dimensional dendrogram is shown in the Supplementary Fig. S1). Nearly identical dendrograms were obtained for both CentHnd and CentXba SNP data (not shown).

**Supervised analysis of SNP array and gene expression data.** The NCI60 cell lines were grouped into two classes based on the presence or absence of amplification at chromosome 3p14-3p13. We then performed supervised analyses using in-triplicate NCI60 gene expression data generated by Novartis on the Affymetrix U95v2 array platform (<http://dtp.nci.nih.gov/mtargets/madownload.html>). An extended description of this approach is presented in the Supplementary Information. To identify genes whose means differed significantly between classes, we performed 500 permutations of class labels using the *t*-test metric. *t* scores and corresponding *P* values were also calculated by standard methods, and *P*-values were adjusted to account for multiple hypotheses, as described in the Supplementary Information.

**Quantitative, real-time PCR.** Quantitative PCR was performed using a SYBR Green kit (Applied Biosystems) and either a PRISM 7500 sequence detector or the PRISM 7300 384-well sequence detector (Applied BioSystems) as described in the Supplementary Information.

**FISH.** Tissue samples used for interphase FISH analysis were derived from a melanoma tissue microarray described elsewhere<sup>28</sup>. BAC clones RP11-584A6 and RP11-444P10 spanning the *MITF* locus were obtained from the Children's Hospital of Oakland Research Institute (CHORI). BAC DNA was prepared with the NucleoBond Plasmid Mini Kit (Clontech). Probe labelling with Digoxin-dUTP (Roche) was performed as described<sup>29</sup>. Centromere probes were obtained from Vysis. The integrity and purity of all probes were verified by hybridization to metaphase spreads before tissue analysis. Tissue hybridization, washing, and bicolour detection were performed as described previously<sup>29</sup>. *MITF* amplification was defined as the presence of four or more gene copies compared to two copies of the chromosome-3 centromere probe in at least 50 nuclei.

**Kaplan–Meier analysis.** Survival curves for 160 metastatic melanoma patients (analysed by FISH as described above) were calculated using Kaplan–Meier analysis with assessment of statistical significance using the Mantel–Cox log-rank test. The Cox proportional-hazards model was used for multivariate analysis to determine relative risk and independent significance. Analyses were performed with Statview 5.0.1 (SAS Institute). Patients were deemed uncensored if they died of melanoma within 5 years of their initial date of diagnosis. Survival was measured from the time of initial diagnosis. Clinicopathologic correlations were determined as described in the Supplementary Information.

**AQUA of MITF protein expression.** AQUA image acquisition and analysis<sup>14</sup> was performed as described in the Supplementary Information.

**Adenoviral vector construction.** The dominant-negative *MITF* construct was generated as described in the Supplementary Information.

**Cell line culture and adenoviral infections.** NCI60 melanoma cell lines (MALME-3M, SK-MEL-5 and UACC257) were obtained from R. Camalier and D. Scudiero (NCI DTP) and were cultured in RPMI containing L-glutamine, 10% fetal bovine serum (FBS; HyClone), and antibiotic/antimycotic (Sigma). For adenoviral infections, 5,000 cells per well were plated in a 96-well plate. After adhering for 6–8 h, adenoviruses described in the text were added at the indicated MOI in serum-free RPMI containing 10 mM MgCl<sub>2</sub> for 30 min at 24 °C. After infection, cells were supplemented with RPMI containing FBS and cultured at 37 °C/5% CO<sub>2</sub> for up to 72 h before subsequent analyses (see below).

**Preparation and retroviral transduction of primary melanocytes.** Isolation, immortalization, and retroviral transduction of primary human melanocytes is described in the Supplementary Information.

**Soft agar assays.** Cells (10,000 per well) were seeded in 0.5% low-melting-point agarose in DMEM with 10% FBS, layered onto 0.8% agarose in DMEM/10% FBS. Colonies were stained with crystal violet, enumerated and photographed at 4 × magnification (40 × microscopy) eight weeks after seeding.

**Pharmacologic data analysis.** Pharmacologic data ( $-\log_{10}[\text{GI}_{50}]$ ) for 42,796 compounds was downloaded from the NCI website and analysed by supervised learning methods as described in the Supplementary Information.  $\text{GI}_{50}$  is defined as the drug concentration achieving 50% growth inhibition relative to untreated cells.

**Drug sensitivity and cell viability assays.** MALME-3M cells were plated at 5,000 cells per well in a 96-well plate and infected at 500 MOI with adenovirus containing dominant-negative *MITF* (as described above). After 12 h, infected cells and controls were incubated with RPMI containing either 20 μM docetaxel or 20 μM cisplatin for 72 h. Cell viability following drug treatment was measured using the MTS-based CellTiter 96-cell proliferation assay (Promega).

Received 1 December 2004; accepted 19 April 2005.

- Lindblad-Toh, K. *et al.* Loss-of-heterozygosity analysis of small-cell lung carcinomas using single-nucleotide polymorphism arrays. *Nature Biotechnol.* **18**, 1001–1005 (2000).
- Lieberfarb, M. E. *et al.* Genome-wide loss of heterozygosity analysis from laser capture microdissected prostate cancer using single nucleotide polymorphic allele (SNP) arrays and a novel bioinformatics platform dChipSNP. *Cancer Res.* **63**, 4781–4785 (2003).
- Mei, R. *et al.* Genome-wide detection of allelic imbalance using human SNPs and high-density DNA arrays. *Genome Res.* **10**, 1126–1137 (2000).
- Zhao, X. *et al.* An integrated view of copy number and allelic alterations in the cancer genome using single nucleotide polymorphism arrays. *Cancer Res.* **64**, 3060–3071 (2004).
- Bignell, G. R. *et al.* High-resolution analysis of DNA copy number using oligonucleotide microarrays. *Genome Res.* **14**, 287–295 (2004).
- Stinson, S. F. *et al.* Morphological and immunocytochemical characteristics of human tumour cell lines for use in a disease-oriented anticancer drug screen. *Anticancer Res.* **12**, 1035–1053 (1992).
- Ross, D. T. *et al.* Systematic variation in gene expression patterns in human cancer cell lines. *Nature Genet.* **24**, 227–235 (2000).
- Roschke, A. V. *et al.* Karyotypic complexity of the NCI-60 drug-screening panel. *Cancer Res.* **63**, 8634–8647 (2003).
- Nishizuka, S. *et al.* Proteomic profiling of the NCI-60 cancer cell lines using new high-density reverse-phase lysate microarrays. *Proc. Natl Acad. Sci. USA* **100**, 14229–14234 (2003).
- Monks, A., Scudiero, D. A., Johnson, G. S., Paull, K. D. & Sausville, E. A. The NCI anti-cancer drug screen: a smart screen to identify effectors of novel targets. *Anticancer Drug Des.* **12**, 533–541 (1997).
- Eisen, M. B., Spellman, P. T., Brown, P. O. & Botstein, D. Cluster analysis and display of genome-wide expression patterns. *Proc. Natl Acad. Sci. USA* **95**, 14863–14868 (1998).
- Golub, T. R. *et al.* Molecular classification of cancer: class discovery and class prediction by gene expression monitoring. *Science* **286**, 531–537 (1999).
- Steingrimsson, E., Copeland, N. G. & Jenkins, N. A. Melanocytes and the Microphthalmia Transcription Factor Network. *Annu. Rev. Genet.* **38**, 365–411 (2004).
- Camp, R. L., Dolled-Filhart, M., King, B. L. & Rimm, D. L. Quantitative analysis of breast cancer tissue microarrays shows that both high and normal levels of HER2 expression are associated with poor outcome. *Cancer Res.* **63**, 1445–1448 (2003).
- Hemesath, T. J., Price, E. R., Takemoto, C., Badalian, T. & Fisher, D. E. MAP kinase links the transcription factor Microphthalmia to c-Kit signalling in melanocytes. *Nature* **391**, 298–301 (1998).
- Price, E. R. *et al.* Lineage-specific signalling in melanocytes. C-kit stimulation recruits p300/CBP to microphthalmia. *J. Biol. Chem.* **273**, 17983–17986 (1998).
- Wu, M. *et al.* c-Kit triggers dual phosphorylations, which couple activation and degradation of the essential melanocyte factor Mi. *Genes Dev.* **14**, 301–312 (2000).
- Loercher, A. E., Tank, E. M., Delston, R. B. & Harbour, J. W. *MITF* links differentiation with cell cycle arrest in melanocytes by transcriptional activation of *INK4A*. *J. Cell Biol.* **168**, 35–40 (2005).
- Carreira, S. *et al.* *Mitf* cooperates with *Rb1* and activates *p21Cip1* expression to regulate cell cycle progression. *Nature* **433**, 764–769 (2005).
- Davies, H. *et al.* Mutations of the *BRAF* gene in human cancer. *Nature* **417**, 949–954 (2002).
- Jafari, M. *et al.* Analysis of ras mutations in human melanocytic lesions: activation of the ras gene seems to be associated with the nodular type of human malignant melanoma. *J. Cancer Res. Clin. Oncol.* **121**, 23–30 (1995).
- Kubo, A. *et al.* The p16 status of tumour cell lines identifies small molecule inhibitors specific for cyclin-dependent kinase 4. *Clin. Cancer Res.* **5**, 4279–4286 (1999).
- McGill, G. G. *et al.* Bcl2 regulation by the melanocyte master regulator *Mitf* modulates lineage survival and melanoma cell viability. *Cell* **109**, 707–718 (2002).

24. Du, J. *et al.* Critical role of CDK2 for melanoma growth linked to its melanocyte-specific transcriptional regulation by MITF. *Cancer Cell* **6**, 565–576 (2004).
25. Chu, W. *et al.* Tyrosinase-related protein 2 as a mediator of melanoma specific resistance to cis-diamminedichloroplatinum(II): therapeutic implications. *Oncogene* **19**, 395–402 (2000).
26. Berger, R. *et al.* Androgen-induced differentiation and tumorigenicity of human prostate epithelial cells. *Cancer Res.* **64**, 8867–8875 (2004).
27. Chen, C. D. *et al.* Molecular determinants of resistance to antiandrogen therapy. *Nature Med.* **10**, 33–39 (2004).
28. Berger, A. J. *et al.* Automated quantitative analysis (AQUA) of HDM2 expression in malignant melanoma shows association with early stage disease and improved outcome. *Cancer Res.* (in the press).
29. Rubin, M. A. *et al.* Overexpression, amplification, and androgen regulation of TPD52 in prostate cancer. *Cancer Res.* **64**, 3814–3822 (2004).

**Supplementary Information** is linked to the online version of the paper at [www.nature.com/nature](http://www.nature.com/nature).

**Acknowledgements** We thank D. Scudiero and R. Camalier for provision of NCI60 cell lines and DNAs, O. Kabbarah and L. Chin for discussions and provision of reagents, F. Chen and C. Ladd-Acosta for excellent technical assistance, L. Ziaugra and S. Gabriel for assistance with the BRAF(V600E) genotyping assay, and M. Loda for expert advice. This work was supported by grants from the National Institutes of Health (L.A.G., M.A.R., D.L.R. and D.E.F.), the Swedish Wenner-Gren Foundation (H.R.W.), the Center of Molecular Medicine, Austrian Academy of Sciences (S.N.W.), the Howard Hughes Medical Institute (T.R.G.), the American Cancer Society (M.L.M.), the Flight Attendant Medical Research Institute (M.L.M.), the Doris Duke Foundation (D.E.F.), the Tisch Family Foundation (W.R.S.), and the Damon Runyon Cancer Research Foundation (W.R.S.).

**Author Information** The GEO accession number is GSE2520. Reprints and permissions information is available at [npg.nature.com/reprintsandpermissions](http://npg.nature.com/reprintsandpermissions). The authors declare no competing financial interests. Correspondence and requests for materials should be addressed to W.R.S. (William\_Sellers@dfci.harvard.edu).